

Hall Effect in the Vortex Lattice of d -Wave Superconductors with Anisotropic Fermi Surfaces

Wataru Kohno, Hikaru Ueki, and Takafumi Kita

Department of Physics, Hokkaido University, Sapporo 060-0810, Japan

On the basis of the augmented quasiclassical theory of superconductivity with the Lorentz force, we study the magnetic field dependence of the charge distribution due to the Lorentz force in a d -wave vortex lattice with anisotropic Fermi surfaces. Owing to the competition between the energy-gap and Fermi surface anisotropies, the charge profile in the vortex lattice changes dramatically with increasing magnetic field because of the overlaps of each nearest vortex-core charge. In addition, the accumulated charge in the core region may reverse its sign as a function of magnetic field. This strong field dependence of the vortex-core charge cannot be observed in the model with an isotropic Fermi surface.

It was shown previously¹⁾ on the basis of a microscopic theory^{2,3)} that the vortex-core charge accumulated by the Lorentz force on supercurrents exhibits a characteristic magnetic-field dependence in two-dimensional s -wave superconductors. Specifically, the charge density at the core center ρ_0 approximately obeys $\rho_0(H) \propto H(H_{c2} - H)$ owing to the competition between the increasing magnetic field H and decreasing pair potential (H_{c2} : upper critical field). We here investigate how this peak structure and charge profile may be affected by two additional factors, i.e., the Fermi surface and energy-gap anisotropies.

The charge redistribution due to the magnetic Lorentz force can be described by the Hall coefficient. It is well known that the Fermi surface curvature plays a crucial role in the signs and magnitudes of the normal Hall coefficient.⁴⁾ Another crucial factor appears for the Hall coefficient of equilibrium superconductors, i.e., the energy-gap anisotropy, which generally introduces temperature dependences of the excitation curvature formed by quasiparticles. Indeed, it was shown previously by model calculations on a $d_{x^2-y^2}$ pairing that both the Hall coefficient in the Meissner state⁵⁾ and the accumulated charge in an isolated vortex core³⁾ strongly depend on the temperature and may change their signs as a function of temperature. With these results, one may naturally expect that the two factors are also important in the magnetic-field dependences of charge profiles in vortex-lattice states. Hence, we here study the charge distribution in the vortex lattice of a clean d -wave superconductor with anisotropic Fermi surfaces.

Our calculations are based on the augmented quasiclassical equations with the Lorentz force in the Matsubara formalism.³⁾ We can divide them into the standard Eilenberger equations⁶⁻¹⁰⁾ and an electric-field equation^{1,3,5)} through an expansion in terms of the dimensionless quasiclassical parameter $\delta \equiv (k_F \xi_0)^{-1} \ll 1$, where k_F is the Fermi wave number and ξ_0 is the coherence length at $T = 0$. These equations can be written as follows.

$$\varepsilon_n f + \frac{1}{2} \hbar v_F \cdot \left(\nabla - i \frac{2e\mathbf{A}}{\hbar} \right) f = \Delta \phi g, \quad (1a)$$

$$\Delta = g_0 \pi k_B T \sum_{n=-\infty}^{\infty} \langle f \phi^* \rangle_F, \quad (1b)$$

$$\nabla \times \nabla \times \mathbf{A} = -i2\pi e \mu_0 N(0) k_B T \sum_{n=-\infty}^{\infty} \langle v_F g \rangle_F, \quad (1c)$$

$$(-\lambda_{TF}^2 \nabla^2 + 1) \mathbf{E} = -i\pi k_B T \mathbf{B} \times \sum_{n=-\infty}^{\infty} \left\langle \frac{\partial g}{\partial \mathbf{p}_F} \right\rangle_F, \quad (1d)$$

with the normalization condition $g = \text{sgn}(\varepsilon_n) \sqrt{1 - f\bar{f}}$. Here $f = f(\varepsilon_n, \mathbf{p}_F, \mathbf{r})$ and $\bar{f} \equiv f^*(\varepsilon_n, -\mathbf{p}_F, \mathbf{r})$ are anomalous quasiclassical Green's functions, $g_0 \ll 1$ is a dimensionless coupling constant responsible for Cooper pairing, μ_0 and ϵ_0 are the vacuum permeability and permittivity, and $\lambda_{TF} \equiv \sqrt{\epsilon_0/2e^2 N(0)}$ is the Thomas-Fermi screening length, respectively. $\langle \cdots \rangle_F$ denotes the Fermi surface average normalized as $\langle 1 \rangle_F = 1$ and $\phi = \phi(\mathbf{p}_F)$ denotes the gap anisotropy normalized as $\langle |\phi|^2 \rangle_F = 1$. Equations (1b) and (1c) are the self-consistency equations for the pair potential $\Delta(\mathbf{r})$ and the vector potential $\mathbf{A}(\mathbf{r})$, respectively. The electric field $\mathbf{E}(\mathbf{r})$ due to the Lorentz force can be obtained from Eq. (1d), which consists of the quasiclassical Green's function g and $\mathbf{B} = \nabla \times \mathbf{A}$, namely, the solutions of the Elienberger equations (1a), (1b) and (1c). Substituting \mathbf{E} into Gauss' law $\rho(\mathbf{r}) = \epsilon_0 \nabla \cdot \mathbf{E}$, we can find the charge distribution.

For the single-particle energy, we adopt the following dimensionless dispersion for a two-dimensional square lattice used for high- T_c superconductors^{5,11)}:

$$\varepsilon_p = -2(\cos p_x + \cos p_y) + 4t_1(\cos p_x \cos p_y - 1) + 2t_2(\cos 2p_x + \cos 2p_y), \quad (2)$$

with $t_1 = 1/6$ and $t_2 = 1/5$, which forms a band over $-4 \leq \varepsilon_p \leq 4$. The structure of the Fermi surface $\varepsilon_p = \varepsilon_F$ is determined by the average electron filling per site n ($0 \leq n \leq 2$); Fig. 1 shows the Fermi surfaces of $n = 0.9$ and $n = 1.95$ for the single-particle energy of Eq. (2). Each of them is given in the extended zone scheme by a singly connected contour around $(p_x, p_y) = (\pi, \pi)$. On the other hand, we express a $d_{x^2-y^2}$ -wave symmetric energy gap as $\phi(\mathbf{p}_F) \propto [(p_{Fx} - \pi)^2 -$

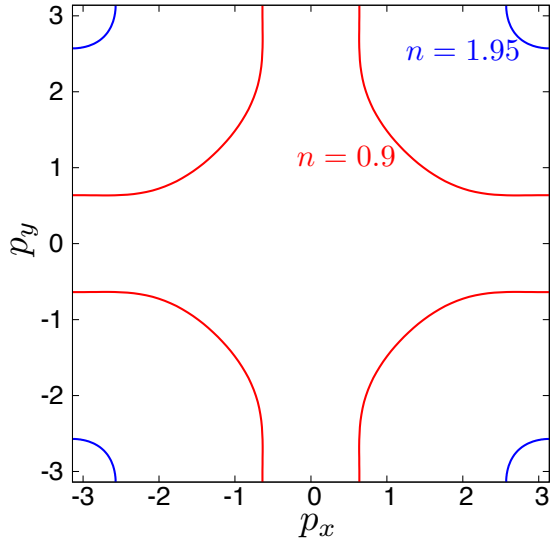


Fig. 1. (Color online) Fermi surfaces of $n = 0.9$ (red line) and $n = 1.95$ (blue line) for the single-particle energy of Eq. (2).

$(p_{Fy} - \pi)^2]$ ($0 \leq p_x, p_y \leq \pi$) which is appropriate for $n \gtrsim 0.8$.

Vortex-lattice solutions of the d -wave superconductor are constructed by using the Eilenberger equations. The corresponding vector potential is expressible in terms of the average flux density $\bar{\mathbf{B}} = (0, 0, \bar{B})$ as $\mathbf{A}(\mathbf{r}) = (\bar{\mathbf{B}} \times \mathbf{r})/2 + \tilde{\mathbf{A}}(\mathbf{r})$,^{12,13} where $\tilde{\mathbf{A}}$ describes the spatial variation of the flux density. Previous studies on the vortex lattice configuration^{14–16} showed that the square lattice state is more stable than the triangular lattice state over a wide range of fields for the $d_{x^2-y^2}$ -wave pairing. Thus, we use the square lattice throughout this analysis. Functions $\tilde{\mathbf{A}}$ and Δ for the square lattice obey the following periodic boundary conditions:^{12,13,17}

$$\tilde{\mathbf{A}}(\mathbf{r} + \mathbf{R}) = \tilde{\mathbf{A}}(\mathbf{r}), \quad (3a)$$

$$\Delta(\mathbf{r} + \mathbf{R}) = \Delta(\mathbf{r}) \exp \left[i \frac{|e|}{\hbar} \bar{\mathbf{B}} \cdot (\mathbf{r} \times \mathbf{R}) + i\pi n_1 n_2 \right], \quad (3b)$$

where $\mathbf{R} = n_1 \mathbf{a}_1 + n_2 \mathbf{a}_2$ with n_1 and n_2 denoting integers, and $\mathbf{a}_1 = a_2(1/2, 1/2, 0)$ and $\mathbf{a}_2 = a_2(0, 1, 0)$ are the basic vectors of the square lattice with the length a_2 determined by the flux-quantization condition $(\mathbf{a}_1 \times \mathbf{a}_2) \cdot \bar{\mathbf{B}} = h/2|e|$.

We follow the numerical procedures shown in Ref. 1 to solve the Eilenberger equations with the boundary conditions in Eq. (3). The convergence of the iteration can be checked by monitoring the free energy of the unit cell. We confirmed that the free energy decreases as the iteration proceeds, which was stopped when the relative difference between the old and new free energies decreased to below 10^{-5} .

We need to obtain H_{c2} to investigate the vortex lattice state in the range $H_{c1} \leq \mu_0 \bar{B} \leq H_{c2}$. In order to obtain H_{c2} corresponding to the present model, we derive an equation for H_{c2} ¹⁸ that incorporates the effects of the Fermi surface and energy-gap anisotropies. To this end, we transform Eqs. (1a) and (1b) into an algebraic equation by expanding Δ and f in the basis function using the solutions of the linearized

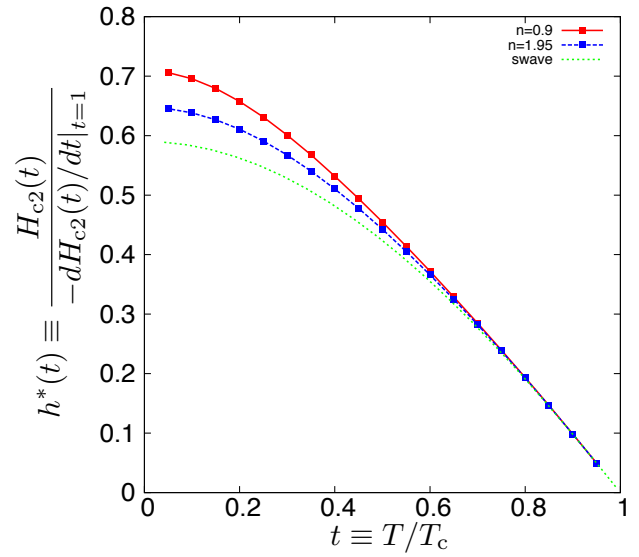


Fig. 2. (Color online) Curves of the reduced critical field $h^*(t)$ for the model of a d -wave superconductor with $n=0.9$ (red solid line with points) and 1.95 (blue dashed line with points) and an s -wave superconductor with a circular Fermi surface (green dotted line).

Ginzburg–Landau equations $\psi_{N,\mathbf{q}}$;

$$\Delta(\mathbf{r}) = \sqrt{V} \sum_{N=0}^{N_{\text{cut}}} \Delta_N \psi_{N,\mathbf{q}}(\mathbf{r}), \quad (4)$$

$$f(\mathbf{r}, \mathbf{p}_F, \varepsilon_n) = \sqrt{V} \sum_{N=0}^{N_{\text{cut}}} f_N(\mathbf{p}_F, \varepsilon_n) \psi_{N,\mathbf{q}}(\mathbf{r}), \quad (5)$$

where $N = 0, 1, 2, \dots$ denotes the Landau level, \mathbf{q} is an arbitrary chosen magnetic Bloch vector characterizing the broken translational symmetry of the vortex lattice and specifying the core locations, and V is the volume of the system. We subsequently take the normal-state limit $g \rightarrow \text{sgn}(\varepsilon_n)$ and $\mathbf{A} \rightarrow \bar{\mathbf{B}} \times \hat{\mathbf{y}}$ in Eq. (1a), substitute Eqs. (4) and (5) into Eqs. (1a) and (1b), multiply them by $\psi_{N',\mathbf{q}}^*$, and perform integrations over \mathbf{r} . Equations (1a) and (1b) are thereby transformed into

$$\sum_{N'} \mathcal{M}_{N,N'} f_{N'} = \phi \Delta_N, \quad (6)$$

$$\Delta_N = g_0 \pi k_B T \sum_{n=-\infty}^{\infty} \langle f_N \phi^* \rangle_F, \quad (7)$$

where \mathcal{M} is a tridiagonal matrix defined by

$$\mathcal{M}_{N,N'} \equiv |\varepsilon_n| \delta_{N,N'} + \beta^* \sqrt{N+1} \delta_{N,N'-1} - \beta \sqrt{N} \delta_{N,N'+1}, \quad (8)$$

with $\beta \equiv \text{sgn}(\varepsilon_n) \hbar v_F e^{-i\varphi_F} / 2 \sqrt{2} l_c$, $\varphi_F \equiv \tan^{-1}(v_{Fy}/v_{Fx})$, and $l_c \equiv \sqrt{\Phi_0 / 2\pi \bar{B}}$. We now introduce the Hermitian matrix $\mathcal{K}_{N,N'} \equiv (\mathcal{M}^{-1})_{N,N'}$ and substitute Eq. (6) into Eq. (7). Then, we obtain the following relation:

$$\left(\Gamma - \pi g_0 k_B T \sum_{n=-\infty}^{\infty} \langle |\phi|^2 \mathcal{K} \rangle_F \right) \Delta \equiv \mathcal{A} \Delta = \mathbf{0}, \quad (9)$$

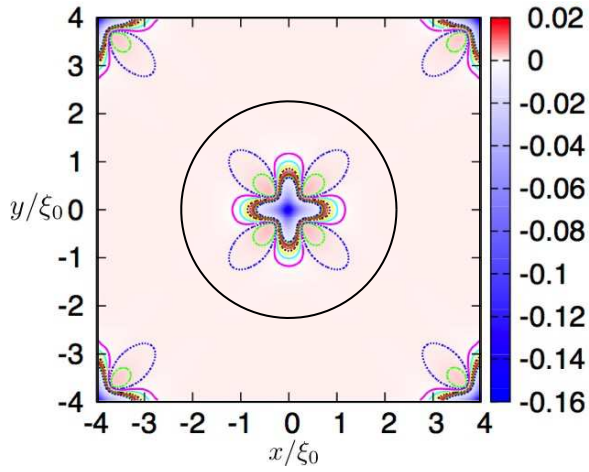


Fig. 3. (Color online) Charge density $\rho(\mathbf{r})/\rho_0$ in the vortex lattice calculated for the case of $n = 1.95$ and $\mu_0 \bar{B}/H_{c2} = 0.022$ over $-a_2/2 \leq x, y \leq a_2/2$, where $a_2/\xi_0 = 8.0$.

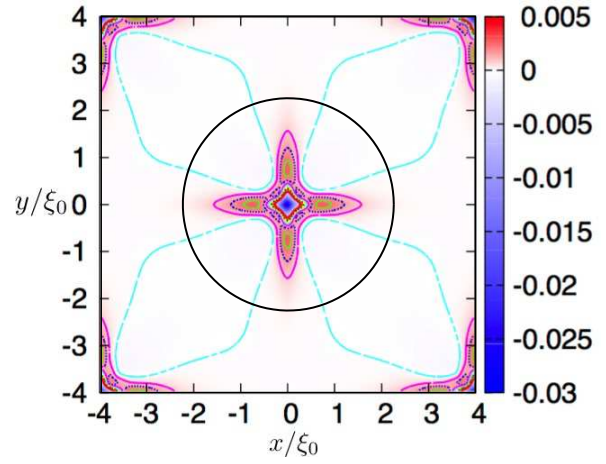


Fig. 5. (Color online) Charge density $\rho(\mathbf{r})/\rho_0$ in the vortex lattice calculated for the case of $n = 0.9$ and $\mu_0 \bar{B}/H_{c2} = 0.018$ over $-a_2/2 \leq x, y \leq a_2/2$, where $a_2/\xi_0 = 8.0$.

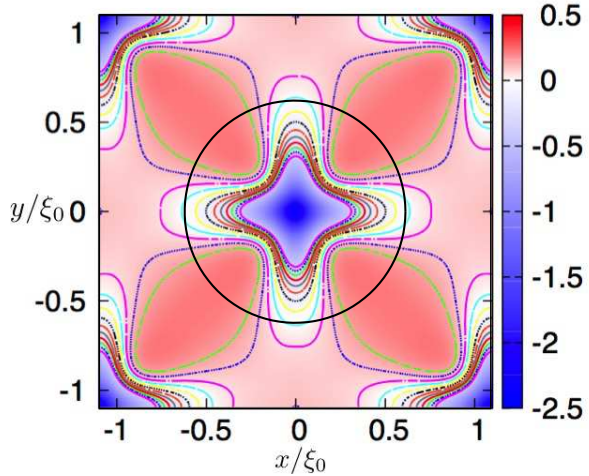


Fig. 4. (Color online) Charge density $\rho(\mathbf{r})/\rho_0$ in the vortex lattice calculated for the case of $n = 1.95$ and $\mu_0 \bar{B}/H_{c2} = 0.29$ over $-a_2/2 \leq x, y \leq a_2/2$, where $a_2/\xi_0 = 2.2$.

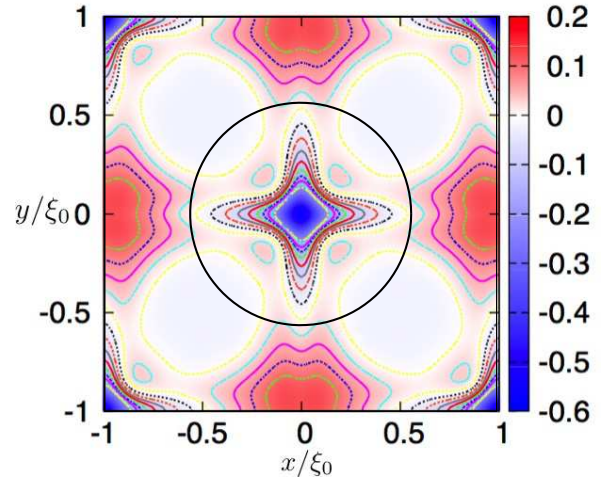


Fig. 6. (Color online) Charge density $\rho(\mathbf{r})/\rho_0$ in the vortex lattice calculated for the case of $n = 0.9$ and $\mu_0 \bar{B}/H_{c2} = 0.29$ over $-a_2/2 \leq x, y \leq a_2/2$, where $a_2/\xi_0 = 2.0$.

where we define Γ as an $N_{\text{cut}} \times N_{\text{cut}}$ unit matrix and $\Delta \equiv (\Delta_0, \Delta_1, \dots, \Delta_{N_{\text{cut}}})^T$. We determined H_{c2} as the largest solution of the equation

$$\det \mathcal{A}(H = H_{c2}) = 0. \quad (10)$$

Equation (9) with the condition in Eq. (10) is an H_{c2} equation that is applicable to clean superconductors with arbitrary energy gaps and Fermi surfaces. Indeed, it reduces to the Helfand–Werthamer theory¹⁹⁾ without impurity scattering by setting ϕ to 1 and using the spherical Fermi surface. It was numerically found for the present $d_{x^2-y^2}$ model that $N_{\text{cut}} = 12$ yields satisfactory convergence at all temperatures. We show the temperature dependence of the reduced critical

field $h^* \equiv (-dH_{c2}/dt|_{t=1})^{-1} H_{c2}(t)$ ($t \equiv T/T_c$) of this model in comparison with the result for a two-dimensional s -wave superconductor in Fig. 2. We see that the energy-gap or Fermi surface anisotropy enhances the value of h^* as the temperature is lowered.

Using the solutions thereby obtained by the standard Eilenberger equations, we numerically calculated the charge density caused by the Lorentz force in the $d_{x^2-y^2}$ vortex lattice. The results presented below were obtained for $T/T_c = 0.3$, $\delta = 0.05$, $\lambda_{\text{TF}}/\xi_0 = 0.05$, and $\lambda_L/\xi_0 \equiv \sqrt{\hbar}/\mu_0 \Delta_0 \xi_0 e^2 N(0) \langle v_F \rangle_F / \xi_0 = 100.0$, where Δ_0 denotes the energy gap at $(H, T) = (0, 0)$. The charge density and total charge in two dimensions are normalized by $\rho_0 \equiv \epsilon_0 \Delta_0 / |e| \xi_0^2$ and $Q_0 \equiv \epsilon_0 \Delta_0 / |e|$, respectively. We also refer to the area $r \leq a_2 / (2\sqrt{\pi}) \approx 0.28a_2 \equiv r_{\text{in}}$ as the *vortex core region* (VCR),

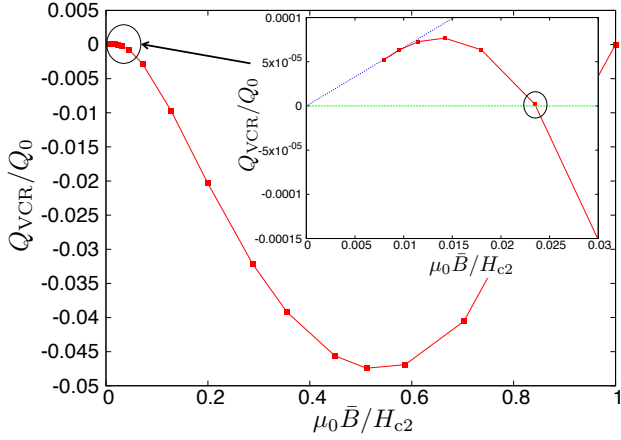


Fig. 7. (Color online) Total charge inside the VCR, Q_{VCR}/Q_0 , as a function of $\mu_0 \bar{B}/H_{c2}$ calculated for the case of $n = 0.9$. The sign reversal of Q_{VCR} can be observed at $\mu_0 \bar{B}/H_{c2} = 0.024$.

which occupies half of the unit cell of the vortex lattice, where $r \equiv \sqrt{x^2 + y^2}$. Circles with a radius of $r = r_{\text{in}}$ are drawn in all figures below in order to visually indicate the VCR.

First, we show the results calculated for $n = 1.95$, where the Fermi surface is almost isotropic. Figures 3 and 4 show the spatial distributions of the charge density at $\mu_0 \bar{B}/H_{c2} = 0.022$ and 0.29, respectively, over the range of $-a_2/2 \leq x, y \leq a_2/2$. In Fig. 3, the fourfold symmetry of the charge density in the vortex core is caused solely by the gap anisotropy since each vortex at $\mu_0 \bar{B}/H_{c2} = 0.022$ is almost isolated.³⁾ As the magnetic field is increased further, the vortex lattice symmetry generally starts to affect the charge distribution owing to the overlapping of vortices.¹⁾ We observe the effect of overlapping clearly in Fig. 4 as compared with in Fig. 3; however, both the fourfold symmetry and the basic charge profile remain invariant. Note that the value of the accumulated charge in the VCR is found to be always negative as a function of magnetic field.

Figures 5 and 6 show the charge profiles at $\mu_0 \bar{B}/H_{c2} = 0.018$ and 0.29, respectively, calculated for the realistic filling of $n = 0.9$ for high- T_c superconductors. In Fig. 5 at $\mu_0 \bar{B}/H_{c2} = 0.018$, the region of the negative charge density extends along the 45° directions far outside the VCR owing to the cooperative effect of the energy gap and Fermi surface anisotropies.³⁾ By increasing the magnetic field, positive charge accumulates at interstitial regions of neighboring vortices owing to their overlapping, as shown in Fig. 6, causing a reduction of the positive charge in the core region. We point out that the change in the charge profile from Fig. 5 to Fig. 6 is much greater than that from Fig. 3 to Fig. 4 at $n = 1.95$. Its origin can be traced to the competition between the energy-gap and Fermi surface anisotropies, which is far more conspicuous at $n = 0.9$.

In figure 7, we show the magnetic field dependence of the accumulated charge $Q_{\text{VCR}} \equiv \int_0^{2\pi} \int_0^{r_{\text{in}}} r \rho(r, \varphi) dr d\varphi$ calculated at $n = 0.9$. We see that $|Q_{\text{VCR}}|$ is enhanced strongly by the

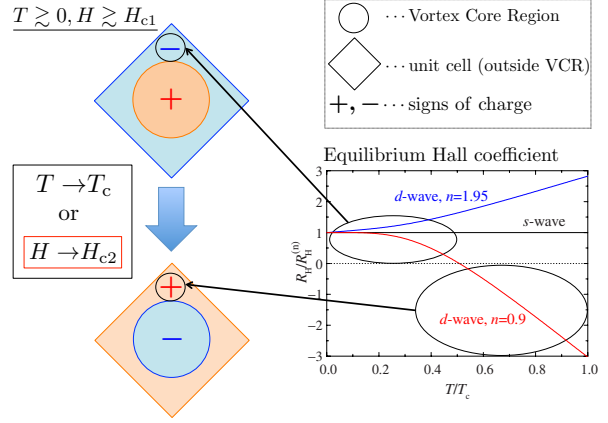


Fig. 8. (Color online) Schematic drawing of the sign reversal of the vortex-core charge for $n = 0.9$ using Fig. 3 in Ref. 5. The normal Hall coefficient $R_H^{(n)}$ is negative for $n = 0.9$. The accumulated charge inside the VCR, Q_{VCR} , has the opposite sign to that outside the VCR owing to the charge neutrality. The accumulated charge outside the VCR may change its sign because the excitation curvature for $H : H_{c1} \rightarrow H_{c2}$ changes similarly to that for $T : 0 \rightarrow T_c$.^{3,5)}

magnetic field with a peak near $H_{c2}/2$. This peak structure, which is characteristic of the Lorentz force mechanism for the charging, originates from the competition between the increasing magnetic field and the decreasing pair potential.¹⁾ The absolute value of this peak can be 10^2 – 10^3 times larger than that for $\mu_0 \bar{B}/H_{c2} \lesssim 0.05$. This feature is commonly seen in our previous study on the s -wave case with an isotropic Fermi surface. However, for the present anisotropic $d_{x^2-y^2}$ pairing on a reasonably anisotropic Fermi surface of $n = 0.9$, we even observe a sign change of Q_{VCR} as a function of magnetic field as seen in the inset of Fig. 7. On the basis of the charge neutrality of the system, we can analyze the sign of Q_{VCR} in terms of the sign of the accumulated charge outside the VCR. A schematic drawing of the sign reversal of the vortex-core charge observed for $n = 0.9$ is shown in Fig. 8. Assuming that $|\Delta|$ is constant to the zeroth order, we may describe the electric field outside the VCR by

$$\mathbf{E} = \mathbf{B} \times \underline{R}_H \mathbf{j}_s, \quad (11)$$

where \underline{R}_H is the equilibrium Hall coefficient tensor in the Meissner state,^{3,5)}

$$\underline{R}_H = \frac{1}{2eN(0)} \left\langle \frac{\partial}{\partial \mathbf{p}_F} (1 - Y) \mathbf{v}_F \right\rangle_F \langle \mathbf{v}_F (1 - Y) \mathbf{v}_F \rangle_F^{-1}, \quad (12)$$

\mathbf{j}_s is the supercurrent, and Y is the Yosida function.²⁰⁾ The Hall coefficient, which determines the sign and magnitude of the carriers in the Meissner state, has the temperature dependence given in Fig. 8, which exhibits a sign change due to the change in the excitation curvature under the growing energy gap as $T \rightarrow 0$. Now, its high-temperature (low-temperature) region may be identified with the high-field (low-field) case in the magnetic-field dependence of the charge accumulation outside the VCR at $T = 0.3T_c$. This identification allows us

to describe the magnetic-field dependence of the charge accumulation and its sign change outside the VCR. Thus, we may conclude that the sign change seen in Fig. 7 as a function of magnetic field is brought about by the change in the excitation curvature under the decreasing pair potential as $\mu_0 \bar{B} \rightarrow H_{c2}$. In this context, we note that the vortex-core charge in an s -wave vortex lattice with a circular Fermi surface has the same sign (positive) with increasing magnetic field since the excitation curvature outside the VCR does not change.

In summary, we have numerically studied the magnetic-field dependence of the vortex-core charge caused by the Lorentz force, focusing our attention on the competition between the energy-gap and Fermi surface anisotropies. We found that the accumulated charge in the VCR may reverse its sign as a function of magnetic field as well as a function of temperature.³⁾ The sign of the vortex-core charge has been discussed²¹⁾ in connection with the anomalous sign change of the flux-flow Hall conductivity^{22–24)} observed in various type-II superconductors. Whether the present mechanism for the sign change is relevant to the sign change of the flux-flow Hall conductivity has yet to be clarified, which will require a detailed calculation of the Hall coefficient in the resistive flux-flow regime.

-
- 1) W. Kohno, H. Ueki, and T. Kita, J. Phys. Soc. Jpn. **85**, 083705 (2016).
 - 2) T. Kita, Phys. Rev. B **64**, 054503 (2001).
 - 3) H. Ueki, W. Kohno, and T. Kita, J. Phys. Soc. Jpn. **85**, 064702 (2016).
 - 4) See, for example, J. M. Ziman, *Electrons and Phonons* (Oxford University Press, Oxford, 1960), p. 486.

- 5) T. Kita, Phys. Rev. B **79**, 024521 (2009).
- 6) N. B. Kopnin, *Theory of Nonequilibrium Superconductivity* (Oxford University Press, New York, 2001).
- 7) R. D. Parks (ed.), *Superconductivity* (Marcel Dekker, New York, 1969).
- 8) T. Kita, *Statistical Mechanics of Superconductivity* (Springer, Tokyo, 2015).
- 9) J. W. Serene and D. Rainer, Phys. Rep. **101**, 221 (1983).
- 10) A. I. Larkin and Y. N. Ovchinnikov, in *Nonequilibrium Superconductivity*, ed. D. N. Langenberg and A. I. Larkin (Elsevier, Amsterdam, 1986) Vol. 12, p. 493.
- 11) H. Kontani, Rep. Prog. Phys. **71**, 026501 (2008).
- 12) T. Kita, J. Phys. Soc. Jpn. **67**, 2067 (1998).
- 13) M. Ichioka, N. Hayashi, N. Enomoto, and K. Machida, Phys. Rev. B **53**, 15316 (1996).
- 14) I. Maggio-Aprile, Ch. Renner, A. Erb, E. Walker, and Ø. Fischer, Phys. Rev. Lett. **75**, 2754 (1995).
- 15) M. Ichioka, A. Hasegawa, and K. Machida, Phys. Rev. B **59**, 8902 (1999).
- 16) A. S. Cameron, J. S. White, A. T. Holmes, E. Blackburn, E. M. Forgan, R. Riyat, T. Loew, C. D. Dewhurst, and A. Erb, Phys. Rev. B **90**, 054502 (2014).
- 17) U. Klein, J. Low Temp. Phys. **69**, 1 (1987).
- 18) T. Kita and M. Arai, Phys. Rev. B **70**, 224522 (2004).
- 19) E. Helfand and N. R. Werthamer, Phys. Rev. Lett. **13**, 686 (1964).
- 20) K. Yosida, Phys. Rev. **110**, 769 (1958).
- 21) D. I. Khomskii and A. Freimuth, Phys. Rev. Lett. **75**, 1384 (1995).
- 22) For an experimental overview and references, see, for example, S. J. Hagen, A. W. Smith, M. Rajeswari, J. L. Peng, Z. Y. Li, R. L. Greene, S. N. Mao, X. X. Xi, S. Bhattacharya, Q. Li, and C. J. Lobb, Phys. Rev. B **47**, 1064 (1993).
- 23) T. Nagaoka, Y. Matsuda, H. Obara, A. Sawa, T. Terashima, I. Chong, M. Takano, and M. Suzuki, Phys. Rev. Lett. **80**, 3594 (1998).
- 24) I. Puica, W. Lang, W. Göb, and R. Sobolewski, Phys. Rev. B **69**, 104513 (2004).